MAGNETIC RESONANCE IMAGING

Present Applications and Projected Developments

Bertil R. R. Persson, Ph.D.
University of Lund, Department of Radiation Physics

INTRODUCTION

History of Clinical NMR Measurements

The first successful demonstration of the phenomenon of nuclear magnetic resonance (NMR), or nuclear induction in solids and liquids, was published almost simultaneously in 1946 by Bloch, Hansen, and Packard (7) working at Stanford University and Purcell, Torrey, and Pound (75) working at Harvard University. The immediate impact of their work was in physics and chemistry, but the applications have steadily widened and recently the application of NMR in medicine has become very exciting.

From the very beginning, the importance of the relaxation times T1 and T2 in NMR had been realized. The first relaxation parameter, T1, is a time constant that reflects the rate at which excited protons exchange energy and equilibrate with the surrounding environment. The other relaxation time, T2, is a constant that reflects the rate at which protons stop their rotation in phase with each other because of the local magnetic fields of adjacent nuclei. Studies of relaxation behavior in solids and liquids give much insight into molecular dynamics (8). These parameters are also of fundamental importance for the contrast between various tissues and organs in medical NMR imaging.

It was early noted by several workers (33,58,74) that the NMR frequency of a given nucleus was, to a small degree, dependent on the chemical form in which the element was present. The NMR spectrum is thus a fingerprint of the chemical compound, which makes NMR spectroscopy a valuable analytical tool for noninvasive chemical analysis of tissues.

https://doi.org/10.1017/S0266462300001501 Published online by Cambridge University Press

Odeblad et al. (70) published the first studies describing the use of NMR in the field of biomedicine. This initial survey included human and rabbit blood fractions; yeast cells; rabbit liver, muscle, and fat; rat liver, muscle, and fat; calf cartilage; human Achilles' tendon; and D_2O. Over the next decade Odeblad's research team continued their NMR studies, and of special interest was their discovery of cyclical hormone-controlled changes in the viscosity of cervical mucus which could be related to a worldwide birth-control effort (54).

Singer (84) demonstrated the use of NMR to measure blood flow. He related the amplitude of an NMR proton signal in the tail of a live mouse to blood flow through the tail's vascular system. This approach is now being coupled with NMR imaging to measure blood flow in arteries and veins and will probably be of large medical significance.

Damadian et al. (30) made the important observation that the relaxation times T1 and T2 were significantly higher in cancerous tissue than in corresponding normal tissue. Moon and Richards (66) reported the first high-resolution ^{31}P-NMR studies of various metabolites in intact blood cells. Recording of a ^{31}P-NMR spectrum from an intact, freshly excised muscle from a rat's leg was first reported by Hoult et al. (51). Since then a wide range of studies on perfused animal hearts, kidneys, livers, and other organs has been pursued, using mainly ^{31}P-NMR, but also ^{1}H and ^{13}C-NMR spectroscopy (39).

It was then a natural step to examine intact living organisms such as bacteria, mice, rats, and rabbits. Eventually, many high-resolution spectra were recorded from the human hand, arm, foot, and leg. In this way it has been possible to monitor the metabolism of both normal and diseased human limbs (39).

Quite recently, the development of 2-Tesla superconducting magnets with access to the whole human body has made it possible to obtain high-resolution NMR spectra from the human body. It may be expected that high-resolution NMR spectroscopy will yield valuable clinical information on almost any part of the human body, especially such organs as the brain, heart, kidney, and liver. Already the technique is used to provide information on the metabolic state of kidneys prior to transplantation.

Another area of NMR's clinical application is NMR-imaging, a distinctly different approach from NMR spectroscopy. In a letter to *Nature*, Lauterbur (59) published the first NMR image of a heterogenous object, namely two tubes of water. He pointed out the simple fact that if a field gradient is applied to a structural object, each nucleus responds with its own NMR frequency determined by its position. Thus applying the gradient in a series of directions and obtaining a series of projections, he used the well-known filtered back-projection technique in about the same way as it is done in computer tomography (CT) X-ray scanning.

Since hydrogen is the most abundant element in all living organisms, proton NMR lends itself particularly well as a method of imaging in biology and medicine; some work has also been done with ^{19}F, ^{23}Na and ^{31}P (5,18,48,49,67,78,89).

The first living human image, that of a finger, was reported in 1976 (62), rapidly followed in 1977 by the hand (2) and the thorax (32). Images of the head and the abdomen were demonstrated in 1978 (26,63). Since then NMR images have immensely improved in quality, in both resolution and tissue discrimination.

A milestone in the history of NMR imaging was the seminal conference at Winston-Salem, North Carolina in 1982 (95). At that time the only machine op-

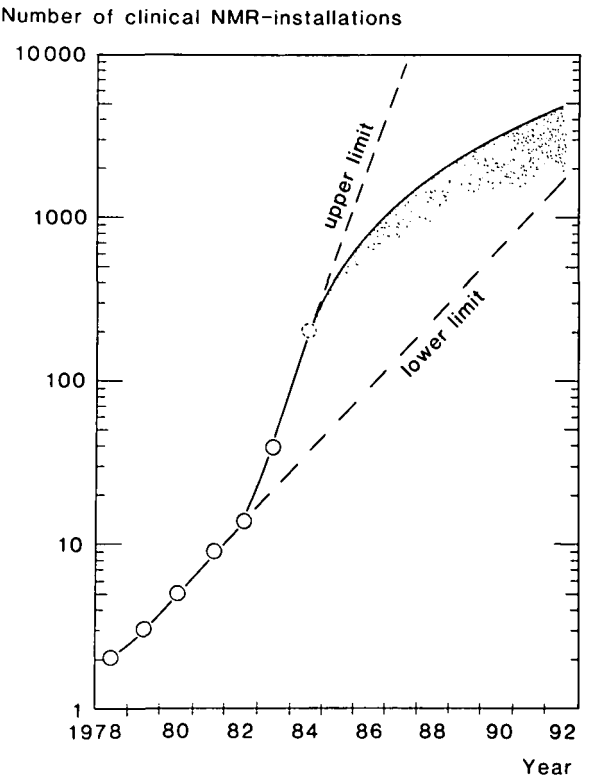

Figure 1. The number of installations of clinical NMR scanners in the world (19). The estimates for the future are based on the experience of CT development.

erating clinically in a hospital, built by EMI Central Research Laboratories and reconstructed by Picker International, was at Hammersmiths Hospital in London. In the Medical Physics Department at Aberdeen University there was another machine which had scanned a number of patients. FONAR Corporation had a machine in the factory development hall which had also scanned patients. Since then the development of clinical use of NMR has grown enormously.

Today there are several commercial companies that have NMR scanners in production. The trend of the number of clinical NMR machines in USA, Europe and Japan is shown in Figure 1 (19). Not only does the *number* of machines increase: the most dramatic changes are in the available image quality and the possibilities of measuring new parameters.

The impact of the first image and the work which followed have been so tremendous that within a decade of its publication manufacturers worldwide have produced NMR scanners generating high-quality images of all parts of the human body that challenge traditional modalities of imaging in clinical practice. Before long, all major hospitals will probably be equipped with NMR scanners.

NMR imaging offers some special advantages over other diagnostic imaging methods used in medicine. First of all, NMR imaging does not use ionizing radiation and would therefore be less hazardous than imaging modalities using X-rays, γ-rays, positrons, or heavy ions. In contrast to ultrasound, the Rf (radio

https://doi.org/10.1017/S0266462300001501 Published online by Cambridge University Press

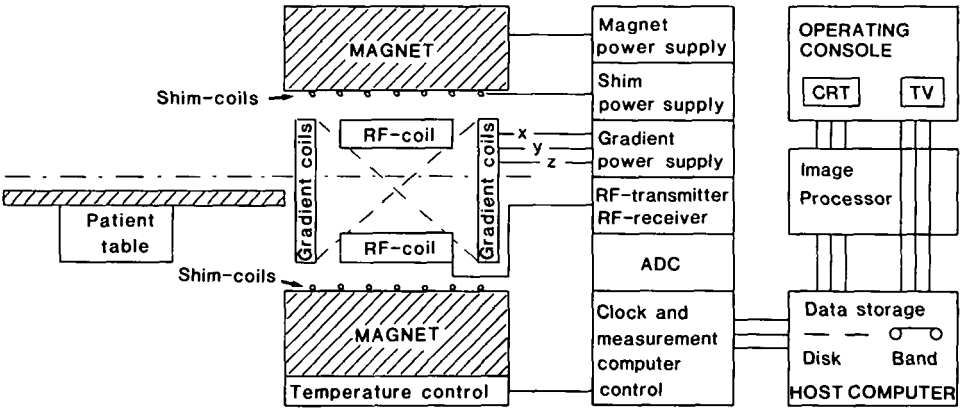

Figure 2. Schematic display of a whole-body NMR scanner. The static field is generated by the large cylindrical coils or permanent magnets. Gradient coils are quadrupoles located at various orientations producing magnetic field gradients in x, y, and z directions. The Rf coil is oriented to produce a magnetic field at a right angle to the static magnetic field.

frequency) radiation used in NMR imaging penetrates bony structures without attenuation. Moreover, besides giving morphological information, NMR imaging gives additional diagnostic insights through relaxation parameters, which are not available from other imaging modalities. Finally, in contrast with CT X-ray scanning, NMR imaging can provide direct 3-D images or of slices of arbitrary orientation such as images of transverse, coronal, or sagittal slices.

Instrumentation for NMR Measurements

A whole-body NMR-scanning machine is shown in Figure 2, where the static magnetic field is generated by large coils or permanent magnets. Dynamic magnetic gradient fields are generated by quadrupoles located at various orientations, producing magnetic gradients in x, y, and z directions. The Rf radiation is transmitted through a coil which also serves as an antenna that receives the NMR signals.

The first generation of NMR scanners was built with a resistive Helmholtz coil configuration producing a field strength about 0.1 Tesla. The maximum field strength which can be reached with resistive magnets based on airwinded coils is about 0.15 Tesla. By using an iron core or shields it is possible to reach about 0.3 Tesla. This is also the present cost limit for the use of permanent magnets.

In order to obtain a better signal-to-noise ratio and better homogeneity in the static magnetic field, high-field superconductive magnets must be used. They must be cooled with liquid helium and surrounded by a cryostat. In NMR spectroscopy, superconductive magnets are used with a field strength up to about 10 Tesla in a small bore for chemical test-tube applications. In whole-body *in vivo* measurements, a bore of about 1 m in diameter is necessary and the field strength is on the order of 1.5–2.5 Tesla for *in vivo* NMR spectroscopy. In most NMR imaging equipment with superconductive magnets, the field strengths are in the order of 0.5–1.5 Tesla (46).

https://doi.org/10.1017/S0266462300001501 Published online by Cambridge University Press

The exitation of the nuclear spin is induced by a pulse of electromagnetic radiation. The relation between the resonance frequency and the applied static magnetic field is given by the well-known Larmor equation:

$$\text{Frequency } (\upsilon) = \text{Constant } (\gamma/2\pi)\cdot\text{Magnetic Field Strength } (B_0)$$
$$\upsilon = (\gamma/2\pi)\cdot B_0$$

The constant $(\gamma/2\pi)$ in this equation is called the *gyromagnetic ratio* and is specific for each atomic nucleus. For hydrogen (^{1}H)—that is, protons—the constant is 42.577 MHz per Tesla, and for phosphorus (^{31}P) it is 17.2532 MHz per Tesla. Thus in a certain static magnetic field it is possible to separate various nuclei by their resonance frequency.

In present medical NMR measurements the proton resonance frequency is the most commonly used. But in future *in vivo* NMR applications, the resonance frequencies of protons, phosphorus, and other nuclei will be used.

Safety Aspects

In medical *in vivo* NMR measurements the patients and the personnel are exposed to combinations of three categories of magnetic and electromagetic fields: (a) static magnetic fields (SMF), (b) dynamic magnetic gradient fields, and (c) radio frequency electromagnetic-radiation fields. Guideline limits of exposure to these fields during clinical NMR measurements are slightly different in various countries (6,14,68,69).

In general there is no known health hazard involved in exposure to static magnetic fields in the range of field strengths <2.5 Tesla used in clinical *in vivo* applications of NMR. Interactions between magnetic fields and pacemakers or metallic implants such as surgical clips in the body, however, might be potentially hazardous, as might be absorption of Rf-power by large implants such as hip prostheses. For diagnostic purposes, the average level of absorbed Rf power in the body must be as low as 0.4 W/kg in order to prevent an increase in body temperature.

In NMR imaging, pulsed gradients are used to produce the spatial resolution. The time of exposure to these dynamic magnetic fields is very short. With rapidly changing gradients, the time dereviative (dB/dt) can be about 1 Tesla per second (T/s) inside magnet. This magnitude is on the borderline where sensations of magnetophosphenes can be experienced. This effect, however, is believed to be without health hazard. Outside the installation, the dynamic magnetic fields are very low and are unable to produce detectable biological effect.

DEVELOPMENTS IN CLINICAL HYDROGEN NUCLEAR MAGNETIC RESONANCE EXAMINATIONS

Clinical ^{1}H-NMR Examinations Compared to Other Diagnostic Modalities

As proton magnetic resonance imaging (^{1}H-NMR) has rapidly evolved into clinical practice, the question of the efficacy of ^{1}H-NMR in comparison to other noninvasive diagnostic techniques has arisen. Below is a brief summary of clinical ^{1}H NMR reflecting its status in fall 1984 as expressed in August at The 3rd Annual

https://doi.org/10.1017/S0266462300001501 Published online by Cambridge University Press

Meeting of The Society of Magnetic Resonance in Medicine in New York, in October at the 1st European Meeting of Nuclear Magnetic Resonance in Medicine and Biology in Geneva, and in November at the RSNA/AAPM Annual Meeting in Washington.

Central Nervous System and Spinal Cord. Brain pathology is well demonstrated by ^{1}H-NMR, particularly using the multi-spin-echo techniques. It is superior to X-ray CT for anatomical description and disease detection in the posterior fossa and brain stem (15,16,99).

Delineation of the tumor by NMR is frequently complicated by edema at the tumor margin, and the metabolic state of the tumor cannot be ascertained by present NMR techniques. Future developments in pulse sequences and contrast agents will probably improve the contrast between tumor and edema.

^{1}H-NMR can detect medium and large vessel blood flow, but it cannot compete with digital subtraction angiography (i.v. or i.a.), the procedure of choice for blood vessel architecture studies (17,81).

For detection of small white matter lesions such as those found in multiple sclerosis and in periventricular regions in aging, NMR is currently superior to all other techniques.

By using the spin-echo technique with a long pulse interval (TR $\approx$ 1500 ms) and a long echo delay (TE $\approx$ 120 ms), differences in tissue signal intensity can be detected based primarily on T2 relaxation differences. Advantages of the T2-weighted image include maximum contrast of most pathologic lesions. In most cases the contrast is nonspecific, but permits differentiation between neoplasms of the sinuses and benign inflamatory retention lesions (40). This technique has also been very useful for detection of most of the pathology that affects the central nervous system (CNS) (12).

Low-field ^{1}H-NMR imaging of intracranial hemorrhage has been shown to be useful for diagnosis in the acute and resolving phases and may offer an opportunity for dating intracerebral hemorrhages (82,83). Further development in the technology of clinical ^{1}H-NMR is needed in order to evaluate the influence of magnetic field strength on image quality, information content, and cost-effectiveness.

Use of intravenous gadolinium-DTPA as a contrast agent in ^{1}H-NMR imaging of the brain shows a high degree of enhancement in cases of both nonmalignant and malignant disease of the brain. Poorly visualized acoustic neuronomas become obvious following administration of Gd-DTPA and peripheral enhancement is seen in infarction. A different pattern of enhancement is also seen in multiple sclerosis and ring enhancement in tuberculoma (17,29).

Tumors generally show strong signal enhancement following administration of Gd-DTPA, whereas normal tissue is not influenced significantly. The advantage of Gd-DTPA in ^{1}H-NMR imaging of brain tumors includes better definition of the borderline of the tumor, an improved differentiation between tumor and edema, and an assessment of the integrity of the blood–brain barrier (38).

Thorax and Lungs. Proton NMR of the thorax has not yet been found to be as efficacious as convential projection and X-ray CT radiology studies. This is due to the decreased signal from the low lung proton density and motion associated with pulsative blood flow and breathing. A prospective study made to compare ^{1}H-NMR and CT for studying broncogenic carcinoma indicated that ^{1}H-NMR and

CT appear approximately equal in both sensitivity and specificity (27). Mediastinal disease is, however, well delineated with NMR, particularly in concert with X-ray CT, because of its ability to differentiate tumor masses from large blood vessels, surrounding soft tissues, and fat.

In patients who had broncogenic carcinoma and had undergone prior irradiation, fibrotic changes had a low signal intensity compared to residual or recurrent tumor. Thus ^{1}H-NMR might be a useful method in selected patients for distinguishing between fibrosis and residual or recurrent tumor (42).

Due to differences in T1 and T2 values, blood is distinguishable from other pleural fluids and thus ^{1}H-NMR might be useful for differentiating between transudative, exudative, and hemorrhagic pleural fluids (76).

New spin-echo techniques and gating methods will improve the clinical use of ^{1}H NMR in examinations of thorax and the lungs.

Cardiovascular System Imaging. NMR provides the following important approaches to the diagnosis of diseases of the cardiovascular system:

a. *Anatomical description without injection of contrast material* is possible because blood flowing in the cardiac chambers and great vessels usually gives no signal;
b. *Tissue characterization* is possible, providing unique information on inflammatory diseases of the pericardium and the ischemic condition of the myocardium through changes in relaxation parameters;
c. *Infarct size and location* is possible because in assessment of therapy ^{1}H-NMR is able to identify wall thinning, regardless of anatomic location; and
d. *Evaluation of arteriosclerosis evolution* is possible by the noninvasive imaging of plaque and arterial wall structure.

In most clinical evaluations of the cardiovascular system, ultrasound, X-ray CT, and nuclear medicine procedures are more practical than and provide similar functional information to NMR. Digital subtraction angiography and ultrasound imaging and velocity measurements are currently superior to NMR for the evaluation of carotid artery disease.

At present the unique potential of NMR lies in its ability to detect inflammatory disease of the pericardium and ischemic heart disease by measuring relaxation parameters (28,34). Future developments in the coordination of cardiac gating and NMR signals with blood flow imaging, however, might change NMR's role in cardiovascular system imaging (34).

Breast Imaging. Mammography is still the preferred method for the study of breast pathology. Proton NMR procedures have a future potential for breast imaging (98). But further study is required to determine whether ^{1}H-NMR examination of the breast can give tissue-specific information (86). By applying both spin-echo and inversion recovery imaging techniques Wang et al. (92) got images which revealed the detailed anatomical structure of the breast. Cysts were easily detected, but cancers were less well defined.

There is still a need for technological research and development in special coil design and tailored pulse sequences (96).

Abdominal Imaging. At present ^{1}H-NMR imaging of the abdomen does not have a role competitive with X-ray CT and other contemporary radiographic pro-

cedures. Recent studies by Heiken et al. (47) indicate, however, that ^{1}H-NMR imaging is capable of demonstrating liver metastases with a degree of accuracy similar to that of CT, and even better than CT in the left liver lobe. Gall bladder function can be evaluated effectively with NMR, and as certain liver diseases have characteristic patterns.

Respiratory gating combined with the use of oral contrast agent significantly improves the diagnostic quality of abdominal ^{1}H-NMR scans and may prove necessary for clinical applications of pancreatic imaging (25). Motion blurring and the need for contrast agents to delineate the lumen of the bowel are problems to be overcome in future developments of abdominal NMR imaging.

The renal cortex, medulla, hilum, and associated blood vessels can be demonstrated by NMR better than by other noninvasive imaging methods. Resolution is low relative to X-ray CT and urographic procedures due to motion associated with breathing and the long time necessary for data collection.

Preliminary studies of renal transplants have revealed that changes attributable to transplant rejection and acute tubular necrosis can be imaged using ^{1}H-NMR (61,77). Dramatic differences have been seen between cyclosporin toxicity and acute rejection, making ^{1}H-NMR imaging most promising in postrenal transplant follow-up (53).

Pelvis Imaging. Proton NMR imaging is superior to all other methods for the delineation of normal anatomy and the presence of pathology in the pelvis. Evaluation of prostatic and urinary tumors as well as retroperitoneal disease is readily provided by NMR (52).

Although ultrasound will remain the primary diagnostic imaging modality for pregnancy, there are several specific indications for using ^{1}H-NMR as an adjunct to ultrasound for obstetrical examinations (94). Growth-retarded fetuses show marked reduction in subcutaneous fat, which indicates that ^{1}H-NMR assessment of fetal tissues may allow earlier and more accurate diagnoses of intrauterine growth retardation (85).

Preliminary results indicate that in general ^{1}H-NMR and CT are comparable in detection of gynecological tumors. But ^{1}H-NMR is slightly superior to CT in evaluating the local extent and determining the cystic nature of a lesion (57).

Musculoskeletal Imaging. The proton NMR signal from compact bone is not detected in imaging procedures. Thus compact bones appear as areas of no signal and artifacts similar to the beam-hardening artifacts of X-ray CT are not seen in NMR images. The fatty bone marrow and spongy bone, however, are detected by NMR.

^{1}H-NMR has superior soft tissue contrast compared to that of conventional radiography and X-ray CT, and it is thus a procedure of great clinical potential for the study of soft tissues and musculotendinal injuries and pathologies such as malignant bone tumors and ischemic necrosis.

^{1}H-NMR has not yet been shown to be superior to X-ray CT for study of lower-back disease. But proton NMR can differentiate the healthy from the diseased nucleus pulposus, and thus it has potential in the early detection and evaluation of lumbosacral spine disorders. The value of NMR relative to nuclear medicine and X-ray CT for detection of osteonecrosis of the hip has not been established, but early evidence indicates that ^{1}H-NMR of the hip may be useful in early detection of osteonecrosis (41).

Investigations of the use of NMR imaging in the examination of the knee has been performed by Li et al. (60). NMR imaging also has applications in the diagnosis preoperative evaluation and follow-up during treatment of bone tumors (37,97). ^{1}H-NMR has high future potential in detection and localization of acute injury of ligaments of the knee (90).

Tissue Type Identification with ^{1}H-NMR Using Relaxation Time Measurements

The signal intensity in ^{1}H-NMR images is a function of proton density, the relaxation times T1 and T2, and the pulse sequence timing used. The ordinary ^{1}H-NMR image thus represents a qualitative image which is evaluated visually in the same way as X-ray images. However, it is possible to evaluate the ^{1}H-NMR images numerically in order to get quantitative values of localized *in vivo* ^{1}H-NMR parameters such as proton density (pH) and the relaxation times T1 and T2. One can either evaluate total images of these parameters or numerical values in a selected region of interest (43,55,65,80).

The calculation of T1 and T2 can be done in a variety of ways. But in order to obtain adequate accuracy, a repetition time on the order of 3 times the value of T1 is necessary for both T1 and T2 determinations. Averaging should not be used at the cost of repetition time until this requirement is met (73).

In the determination of T1, a rational choice of the pulse sequence to be employed, the number of images to be generated, the spacing of the variable timing parameter, and the form of the fitting algorithm must be made with consideration of the resultant accuracy in measurement and the net imaging time required. In addition, other constraints of the system such as the spatially inhomogeneous Rf field must be incorporated into the decision process. Taking into account experimental accuracy, the uni-exponential model constitutes an adequate description of the water proton spin-lattice relaxation curves of necrotic tissue only (4). Tumor tissue, liver, kidney, spleen, muscle, and salivary gland tissues show a weak bi-exponentiality, while the eye lens, testes, and fatty tissue show a particularly clear bi-exponentiality. Thus, for future quantitative ^{1}H-NMR imaging, multiexponential models might be proposed.

Correlative studies of NMR relaxation times T1, T2, and histopathological findings in different types of human brain tumors were undertaken by Englund et al. (36) and Györffy-Wagner et al. (44). The gliomas all showed higher T1 values than normal white matter. T2 values were also generally higher than for normal white matter, from which the gliomas usually originate. The peritumorous, edematous tissue had lower T1 values than the tumors, while T2 values varied. Relaxation times for the meningiomas and the metastases fell within the range of normal gray matter. The acoustic neurinomas consistently had T1 and T2 values close to and below the lowest normal gray matter values, respectively.

The information of proton density and relaxation times can be used for tissue type identification by creating a template that contains a list of the tissues that may be found in the section along with the expected distributions of T1, T2, and proton density (72).

The next step is to use a processing algorithm to compare the template and identify which types of tissue correspond to the distribution for the specific region.

https://doi.org/10.1017/S0266462300001501 Published online by Cambridge University Press

Recent developments in methods applying artificial intelligence with statistical pattern recognition use a theorem that recognizes two types of classes. For example *tumor* and *cerebral edema* can be considered as classes: *only* class would be *tumor* not *cerebral edema* while the *complex* class is *tumor* and *cerebral edema*. A decision space is recognized where there exists a hierarchy of levels from feature values to complex classes (87).

Due to the complexity inherent in the multiparametric analysis of ^{1}H-NMR images it would be highly desirable to use a method of artificial intelligence to help experts recommend the examination parameters or evaluate the examination.

The Design of Contrast Agents for ^{1}H-NMR Imaging

Introduction. Trace amounts of paramagnetic metal ions have been shown to reduce the T1 relaxation time of nuclei in the surrounding environment because of the strong electron-nuclear magnetic moment interaction. This property can be utilized advantageously in the development of contrast agents that would be used to shorten the spin-lattice relaxation time T1 in specific tissues or organs.

The change in T1 values produced by paramagnetic ions is determined by the effective magnetic moment of the ion and the average distance between the paramagnetic ion and the hydrogen atoms. The most interesting ions that have been considered as contrast agents are gadolinium(III), manganese(II), iron(III), chromium(III), and copper(II) (64).

Since oxygen is paramagnetic, because of its unpaired electrons, increasing the oxygen concentration in solution causes a decrease in T1. Differences in oxygen saturation of tissue are detectable by ^{1}H-NMR and may therefore be used in studies of infarcted tissues (45).

An alternative approach is to use ferromagnetic particles, which has been found to reduce the T2 relaxation time (71).

Gadolinium-DTPA. Gadolinium-DTPA is an effective intraveneous contrast agent which has been found useful in ^{1}H-NMR imaging and which has no known side effects. It is particularly useful in delineating cerebral tumors from surrounding edema. It has also been found to be of value in enhancing liver tumors as well as other tumors in the abdomen and pelvis (20,21).

Animal experiments have demonstrated further applications of Gd-DTPA, such as permitting the assessment of renal function, detection of changes of differences in tissue vascularity, identification of breakdown of the blood–brain barrier, and improved diagnosis of myocardial ischemia (23,24).

Manganese. Manganese(II) is a strong paramagnetic agent which has been suggested as intravascular NMR contrast agent (79). It has also been shown that manganese sulfide colloids can reduce the T1 relaxation time in liver and lungs (22). The clinical use of the manganese(II) ion, however, may be limited due to the prolonged retention within the body and its toxicity.

Iron Compounds as NMR Contrast Agents. The ferric ion (Fe^{3+}) is a paramagnetic agent which in the form of ferric-ammonium-citrate (5 mM) can be used with apparent safety as a NMR contrast agent for the gastrointestinal tract (13).

Iron oxide (magnetite Fe_3O_4) particles with a diameter of about 0.01 μm embedded in microspheres (diameter 1 μm) made of a matrix of polymerized dextrins are effectively trapped by the reticulo-endothelial system (RES). Since

each magnetite particle acts as a single magnetic domain, the microsphere will strongly alter the local magnetic field which gives an accelerated dephasing of local spins. It has been shown that there is a marked reduction of the T2 relaxation time in rat liver after administration of magnetite-dextrin microspheres (71). Larger microspheres might be used for perfusion studies in the lungs and other organs.

Application of Chemical Shift in Clinical Examinations

The high concentration of water in biological entities is the major advantage of proton NMR imaging. Another chemical species of significant concentration containing hydrogen is lipids. But for most other species, such as metabolites and proteins, water has an almost 10,000 times greater signal than other compounds.

The separation of water (H_2O) and lipids ($-CH_2- \cdots -CH_3$) in the chemical shift spectrum is about 3.5 ppm and thus can be resolved only in an NMR system with high homogeneity. In such a system, however, it is possible to generate

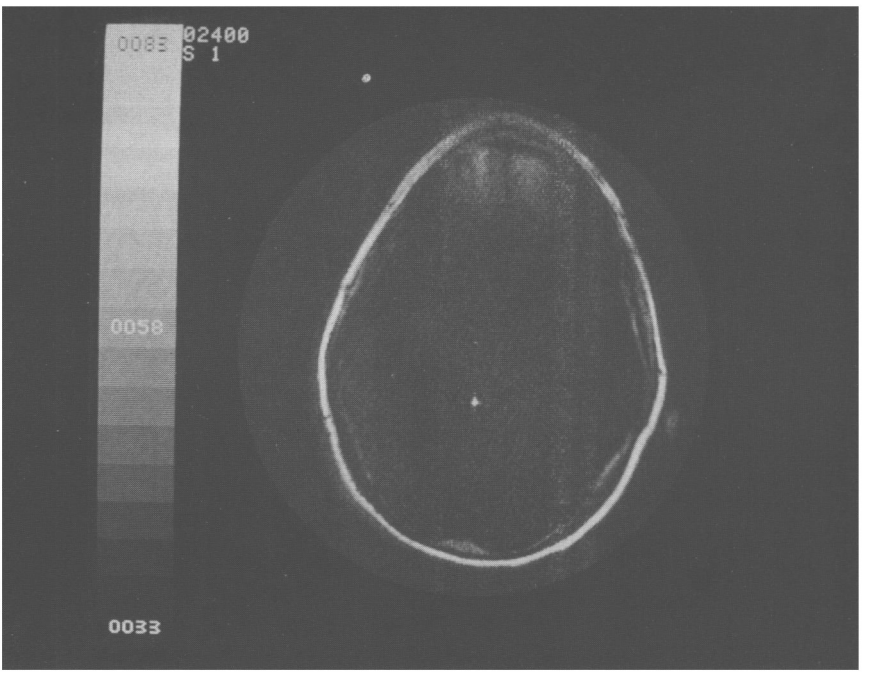

(A)

Figure 3. Chemical imaging of the brain by NMR (9,10): (A) $-CH_2$ chemical image formed by selective irradiation of the H_2O signal before application of conventional imaging sequence. The irradiation pulse is precisely tuned to H_2O resonance and lasts 30 ms. H_2O "signal" near top is a field inhomogeneity artifact; the white spot in center is also an artifact. (B) H_2O chemical image formed by prior irradiation of the $—CH_2$ resonance. (C) Conventional ^{1}H-NMR image obtained with the chemical selective irradiation pulse turned off. All imaging, gain, and display parameters are otherwise the same throughout. (*Reproduced with permission of the author and* The Lancet.)

https://doi.org/10.1017/S0266462300001501 Published online by Cambridge University Press

(B)

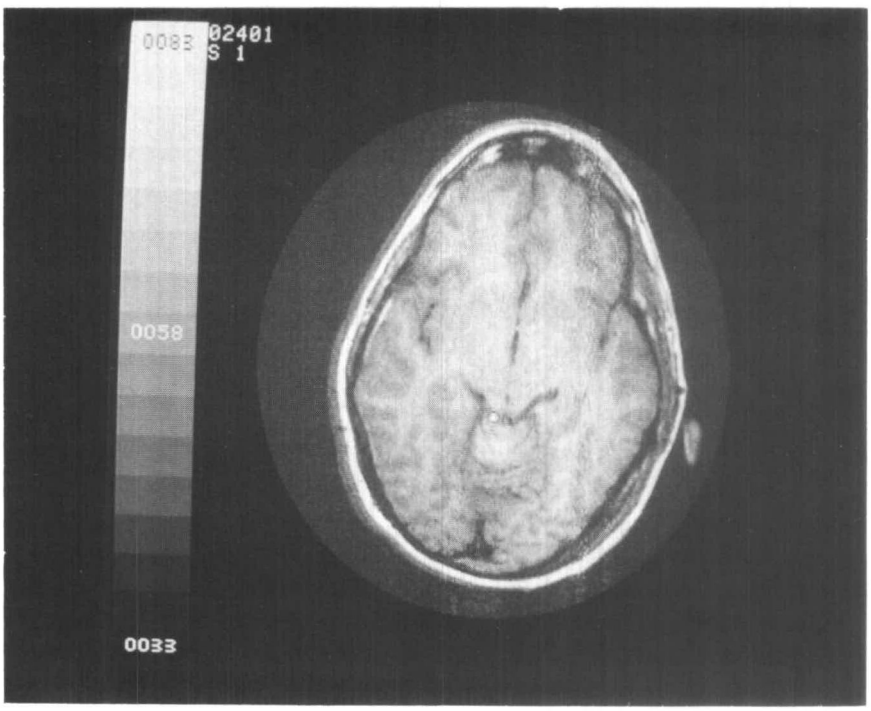

(C)

Figure 3. (*cont.*)

https://doi.org/10.1017/S0266462300001501 Published online by Cambridge University Press

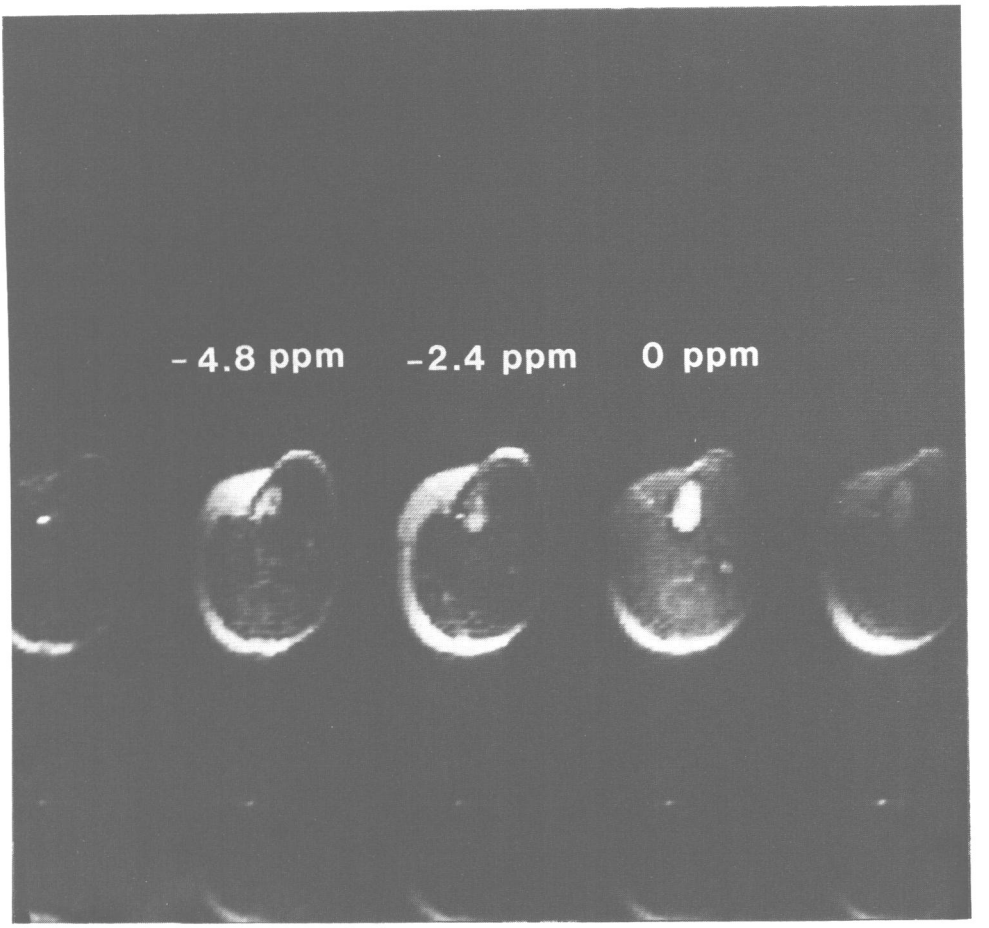

Figure 4. Demonstration of bone marrow involvement with proton chemical shift imaging (82). The figure shows a chemical shift image of a patient suffering from chronic myeloid leukemia. Subcutaneous fat has the highest intensity in the subimage of −4.8 ppm, but the bone marrow and muscle tissue have the highest intensity in the subimage of 0 ppm. (*Reproduced with permission of the author and Raven Press.*)

separate images of water and lipids. Clinical studies are underway which will evaluate the utility of this technique and determine if variations in lipid or water concentrations are manifest in pathology (11,50,82). Figure 3 shows an example of chemical imaging of the brain by NMR (9) and Figure 4 shows chemical shift images of the bone marrow of a patient suffering from chronic myeloid leukemia.

Figure 5 shows images taken from the spine of a normal volunteer by adding a delay Δt to a spin-echo pulse sequence in group 2, adjusted so that $\Delta t \cdot \upsilon = \frac{1}{2}$ ($\Delta\upsilon$ is the chemical shift between protons in water and fat) (35,88). The lower pair of images are images of "fat" and "water" obtained by amplitude or domain subtraction.

https://doi.org/10.1017/S0266462300001501 Published online by Cambridge University Press

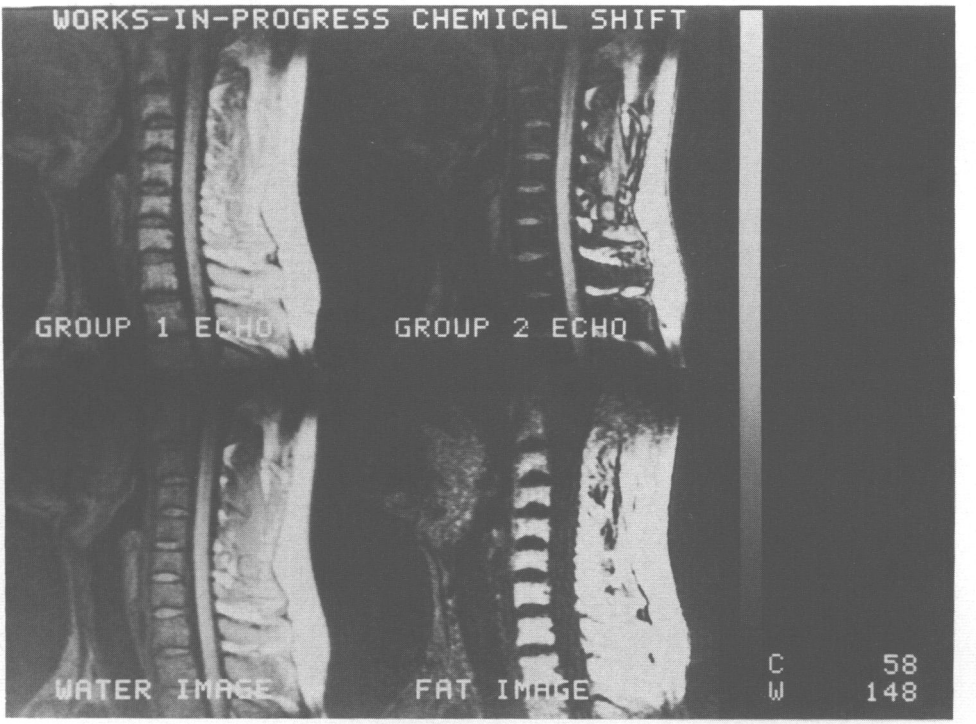

Figure 5. The figure shows images taken from the spine of a normal volunteer by adding a delay Δt to a spin-echo pulse sequence in group 2 adjusted so that $\Delta t \cdot \upsilon = \frac{1}{2}$ ($\Delta\upsilon$ is the chemical shift between protons in water and fat) (35, 88). The lower pair of images is of "fat" and "water" obtained by amplitude or domain subtraction. (*Reproduced with permission of Technicare Corporation.*)

Clinical Application of NMR Flow Imaging

Although the clinical applications of NMR flow imaging are still in their infancy, it appears exceptionally suitable to assess the velocity and profiles of blood flow *in vivo*. Based on the results which so far demonstrate the potential of the technique, it appears that images of both venous and arterial flow can be obtained. In the future, images comparable to angiography might be obtained. In addition, it is now possible to study hemodynamics by NMR.

NMR flow imaging may be useful in a variety of pathologic conditions as a screening and/or adjunctive imaging technique. According to Kaufman et al. (56), Vinocur (91), and van As et al. (3), the clinical applications in the future might include the following:

- obstructions in vessels (plaques, clot, atherosclerotic lesions)
- evaluation of graft patency
- diagnosis of pulmonary arterial and venous hypertension
- identification of pulmonary embolism
- measurement of perfusion of tissue and organisms
- comparison of left and right side blood flow

https://doi.org/10.1017/S0266462300001501 Published online by Cambridge University Press

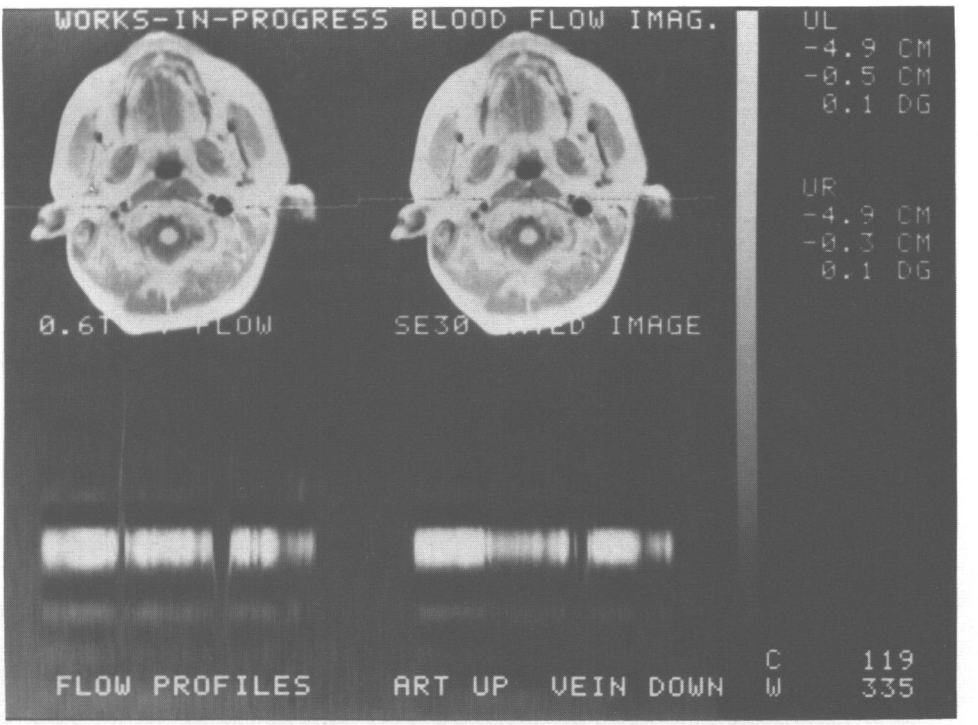

Figure 6. The figure shows arterial flow images of the head taken with cardiac gating. Flow profiles through the vessels indicate differences in arterial and venous flow (88). (*Reproduced with permission of Technicare Corporation.*)

- diagnosis of congenital or acquired heat disease
- detection of impaired motion of heart walls

In some clinical applications of flow imaging, qualitative or semiquantitative blood flow measurements may be sufficient, using a relative scale which relates the NMR intensity of flowing fluid to that found for stationary spins.

Arterial flow imaging using data acquisition synchronous with the cardiac cycle has been reported (93). This procedure however, is time consuming, and in the future direct NMR flow imaging is expected to be developed for real-time imaging of arterial flow (34). Figure 6 shows arterial flow images of the head taken with cardiac gating. Flow profiles through the vessels indicate differences in arterial and venous flow (88).

The assessment of tissue perfusion is becoming increasingly important since medical research is becoming interested in cellular activity. The viscosity and proton relaxation properties of blood depend on the size of the vessels. Therefore perfusion data based on proton flow imaging may be difficult to obtain in a reliable form, particularly when the vessel diameter is less than 0.5 mm (3).

REFERENCES

1. Akin, E. W., Ennis, J. T., Subbiondo, R., Thomas, K., Fitzsimmons, J., Hill, J., Hamlin, D., Mareci, T., Scott, K., & Williams, C. Complementary role of MR imaging and phase analysis in assessment of myocardial damage. *Radiology*, 1984, 153, 261.

https://doi.org/10.1017/S0266462300001501 Published online by Cambridge University Press

2. Andrew, E. R., Bottomley, P. A., Hinshaw, W. S., Holland, G. N., Moore, W. S., & Simaroj, C. NMR images by multiple sensitive point method: Application to larger biological systems. *Physical Medical Biology*, 1977, 22, 971–74.
3. van As, Schaafsma, T. J., de Jager, P. A., & Kleijn, J. M. Flow imaging by nuclear magnetic resonance. *Annals de Radiologie*, 1984, 27, 405–13.
4. Bakker, C. J. G., & Vriend, J. Multiexponential water proton spin-lattice relaxation in biological tissues and its implication for quantitative NMR imaging. *Physical Medical Biology*, 1984, 29, 509–18.
5. Bendel, P., Lai, C. M., & Lauterbur, P. C. ^{31}P Spectroscopic zeugmatography of phosphorous metabolites. *Journal of Magnetic Resonance*, 1980, 38, 343–56.
6. BGA. Bundesgesundheitsamt. Empfehlungen zur vermeidung gesundlicher Risiken verursacht durch magnetisch und hochfrequente elektromagnetische felder bei der NMR-tomographie und in-vivo NMR spectroskopie. *Bundesgesundheitsbl*, 1984, 27, 92–96.
7. Bloch, F., Hansen, W. W., & Packard, M. E. Nuclear induction. *Physical Review*, 1946, 69, 127.
8. Bloembergen, N., Purcell, E. M., & Pound, R. V. Relaxation effects in nuclear magnetic resonance absorption. *Physical Review*, 1948, 73, 679–712.
9. Bottomley, P. A., Foster, T. H., & Leue, W. M. Chemical imaging of the brain by NMR. *The Lancet*, 1984a, May 19, 1120.
10. Bottomley, P. A., Foster, T. H., & Leue, W. M. ^{1}H chemical shift imaging of the brain. *Proceedings of the 3rd Annual Meeting of the Society of Magnetic Resonance in Medicine*, 1984b, 72–73.
11. Bottomley, P. A., Edelstein, W. A., Leue, W. M., Redington, R. W., Schenck, Foster, T. B., & Smith, L. S. Technical feasibility of clinical ^{1}H imaging and ^{31}P spectroscopy. *Proceedings of the 3rd Annual Meeting of the Society of Magnetic Resonance in Medicine*. 1984, 68–69.
12. Brant-Zawadzki, M. Clinical MRI of the CNS: General neurological disorders. *Proceedings of the 3rd Annual Meeting of the Society of Magnetic Resonance in Medicine*, 1984, 88–91.
13. Brasch, R. C. Applications for paramagnetic MRI contrast agents. *Proceedings of the 3rd Annual Meeting of the Society of Magnetic Resonance in Medicine*, 1984, 94–97.
14. BRH, FDA (Bureau of Radiological Health, Food and Drug Administration). *Guidelines for evaluating electromagnetic risk for trials of clinical NMR systems*. Rockville, Md.: FDA, 1982, HFX-460.
15. Budinger, T. F. Comparison of NMR to other modalities. *Proceedings of the 3rd Annual Meeting of the Society for Magnetic Resonance in Medicine* 1984, 115–19.
16. Bydder, G. M. Magnetic resonance imaging of tumors of the central nervous system. *Proceedings of the 3rd Annual Meeting of the Society of Magnetic Resonance in Medicine*, 1984, 122–23.
17. Bydder, G. M., Brown, J., Steiner, R. E., & Young, I. R. Use of intravenous gadolinium-DTPA as a contrast agent in MR imaging of non-malignant disease of the brain. *Radiology*, 1984, 153, 84.
18. Cady, E. B., de L. Costello, A. M., Dawson, J. M., Delphy, D. T., Hope, P. L., Reynolds, E. O. R., Tofts, P. S., & Wilkie, D. R. Non-invasive investigation of cerebral metabolism in newborn infants by phosphorous NMR spectroscopy. *The Lancet*, 1983, May 14, 1059–62.
19. Carlsson, L. (1985) Personal communication.
20. Carr, D. H., Steiner, R. E., & Young, I. R. Initial clinical experience with gadolinium-DTPA as a contrast agent in magnetic resonance imaging. *Proceedings of the 3rd Annual Meeting of the Society of Magnetic Resonance in Medicine*, 1984, 136–37.

21. Carr, D. H., Brown, J., Bydder, G. M., Steiner, R. E., Weinmann, H.-J., Speck, U., Hall, A. S., & Young, I. R. (1984) Gadolinium-DTPA as a contrast in MRI: Initial clinical experience in 20 patients. *American Journal of Radiology*, 143, 215–44.
22. Chilton, H. M., Jackels, S. C., Hinson, W. H., & Ekstrand, K. E. Use of paramagnetic substance, colloidal manganese sulfide, as an NMR contrast materials in rats. *Journal of Nuclear Medicine*, 1984, 25, 604–7.
23. Clanton, J. A., Runge, V. M., Price, A. C., Herzer, C. J., Wehr, V. W., Schorner, R., Felix, R., Partain, C. L., & James, Jr., A. E. Contrast enhanced magnetic resonance imaging of the brain: Experimental and clinical investigation with Gd-DTPA. *Proceedings of the 3rd Annual Meeting of the Society of Magnetic Resonance in Medicine*, 1984, 157–58.
24. Clanton, J. A., Runge, V. M., Price, A. C., Wehr, C. J., Herzer, W. A., Dennis, R. L., Partain, C. L., James, Jr., A. E. Defining the potential of Gadolinium-DTPA, a proposed i.v. contrast agent, in magnetic resonance imaging. *Proceedings of the 3rd Annual Meeting of the Society of Magnetic Resonance in Medicine*, 1984, 159–160.
25. Clanton, J. A., Runge, V. M., Carrol, F. E. Partain, C. L., & James, E. A. The use of oral contrast and respiratory gating in MR imaging of the pancreas. *Radiology*, 1984, 153, 159.
26. Clow, H., & Young, I. R. Britain's brains produce first NMR scan. *New Scientist*, 1978, 88, 588.
27. Cohen, A. M., Creviston, S., Lipuma, J. P., Bryan, P. J., Lieberman, J. M., Guyton, S. W., Clayman, J., Haaga, J. R., & Alfidi, R. J. Comparison of MR and CT for staging Bronchogenic carcinoma. Radiology, 1984, 153, 209.
28. Crooks, L. E., Barker, B., Chang, H., Feinberg, D., Hoeninger, J. C., Watts, J. C., Arakawa, M., Kaufman, L., Sheldon, P. E., Higgins, C. & Botvinick. Strategies for gated MRI of the heart. *Proceedings of the 3rd Annual Meeting of the Society of Magnetic Resonance in Medicine*, 1984, 171–72.
29. Curati, W. L., Steiner, R. E., Kingsley, D. E. P. MR imaging in the diagnosis of acoustic neuronomas. *Radiology*, 1984, 153, 110.
30. Damadian, R. V. Tumor detection by nuclear magnetic resonance. *Science*, 1971, 171, 1151–53.
31. Damadian, R. V. *Apparatus and method for detecting cancer in tissue*. U.S. Patent 3789932, filed 17 March, 1972.
32. Damadian, R. V., Goldsmith, M., & Minkoff, L. NMR in cancer: FONAR image of the live human body. *Physiol Chem Phys*, 1977, 97–108.
33. Dickinson, W. C. Dependence of the ^{19}F nuclear resonance position on chemical compound. *Physiology Review*, 1950, 77, 736–37.
34. van Dijk, P. Direct cardiac NMR imaging of heartwall and blood flow velocity. *Journal of Computer Assisted Tomography*, 1984, 8, 429–36.
35. Dixon, W. T., Faul, D. D., Gado, M. H., Lee, J. K. T., & Murphy, W. A. Using the chemical shift difference between water and lipid in proton imaging. *Radiology*, 1984, 153, 65.
36. Englund, E., Brun, A., Cronquist, S., Györffy-Wagner, Z., Larsson, E.-M., Owman, T., Persson, B. Brain tumours: A correlative study of magnetic resonance and histopathological findings. *Proceedings of the 3rd Annual Meeting of the Society of Magnetic Resonance in Medicine*, 1984, 218.
37. Falke, T. H. M., Bloem, J. A., Taminiau, A. H. M., Doornbos, J., van Oosterrom, A. T. Application of MRI in diagnosis and follow-up during treatment of bone tumors. *Proceedings of the 3rd Annual Meeting of the Society of Magnetic Resonance in Medicine*, 1984, 225–26.
38. Felix, R., Schoerner, W., Claussen, C., Fiegler, W., & Niendorf, P. Diagnostic value of gadolinium-DTPA in MR imaging of brain tumors. *Radiology*, 1984, 153, 84.

39. Gadian, D. G. *Nuclear magnetic resonance and its application to living system*. Oxford: Clarendon Press, 1982.
40. Gado, M. H., Dixon, W. T., Teng, M., Hodges, F. J., & Sartor, K. J. Optimal pulse parameters in spin-echo imaging of brain and spinal cord. *Radiology*, 1984, 153, 141.
41. Genant, H. K., Richardson, M. L., Heller, M., Helms, C. A., & Chafetz, N. I. Magnetic resonance imaging of the musculoskeletal system. *Proceedings of the 3rd Annual Meeting of the Society of Magnetic Resonance in Medicine*, 1984, 259–62.
42. Glazer, H. S., Lee, J. K. T., Levitt, R. G., Totty, W. G., Emami, B., Wasserman, T., & Murphy, W. A. MR imaging of post-treatment fibrosis. *Radiology*, 1984, 153, 209.
43. Gore, J. C., Doyle, F. H., Pennock, J. M. Relaxation rate enhancement observed *in vivo* by NMR imaging. In C. L. Oartain, A. E. James, F. D. Rollo, & R. R. Price (eds.), *Nuclear magnetic resonance imaging*. Philadelphia: WB Saunders, 1983, 94–106.
44. Györffy-Wagner, Z., Englund, E., Larsson, E.-M., Brun, A., Cronquist, S., Owman, T., & Persson, B. (1985) In M. A. Hopf & G. M. Bydder (eds.), *Magnetic Resonance Imaging and Spectroscopy*. Geneva, Switzerland: European Society of Magnetic Resonance in Medical Biology, 1985, 51–55.
45. Hanley, P. Magnets for medical applications of NMR. *British Medical Bulletin* 1984, 40, 125–31.
46. Hart, H. R., Bottomley, P. A., Edelstein, W. A., Karr, S. G., Leue, W. M., Mueller, O., Redington, R. W., Schenck, J. F., Smith, L. S., & Vatis, D. Nuclear magnetic resonance imaging contrast-to-noise ratio as a function of strength of magnetic field. *American Journal of Radiology*, 1983, 141, 1195–1201.
47. Heiken, J. P., Lee, J. K. T., Ling, D., & Glazer, H. S. MR imaging of hepatic metastases. *Radiology*, 1984, 153, 265.
48. Hilal, S. K., Farby, M., Segebatrth, C., Wittekoek, S., & Ra, J. B. *In vivo* and *in vitro* chemical shift imaging of sodium. *Proceedings of the 3rd Annual Meeting of Society of Magnetic Resonance in Medicine*. 1984, 322.
49. Hilal, S. K., Lee, S., Cho, Z. H., Mun, S. K., Ra, J. B., Mawad, M., Silver, A. J., & Sane, P. Proton and sodium NMR in stroke. *Proceedings of the 3rd Annual Meeting of the Society of Magnetic Resonance in Medicine*, 1984, 323.
50. Hilal, S. K., Ra, J. B., Cho, Z. H., Mun, S. K., Mawad, M., Silver, A. J., & Wittekoek, S. Clinical application of proton chemical shift imaging. *Proceeding of the 3rd Annual Meeting of the Society of Magnetic Resonance in Medicine*, 1984, 324.
51. Hoult, D. I., Busby, S. J. W., Gadian, D. G., & Seeley, P. J. Observations of tissue metabolites using ^{31}P nuclear magnetic resonance. *Nature*, 1974, 252, 285–87.
52. Houston, L. W., Turski, P. A., Perman, W. H., Strother, C. M., Hald, J. K., Hayes, C. E., Glover, G., & Wehrli, F. W. *In-vivo* sodium MR imaging: Clinical experience and an experimental canine gliosarcoma model. *Proceedings of the 3rd Annual Meeting of the Society of Magnetic Resonance in Medicine*, 1984, 344.
52a. Hricak, H. Pelvis: Male and female. *Proceedings of the 3rd Annual Meeting of the Society of Magnetic Resonance in Medicine*, 1984, 345.
53. Hricak, H., Pedusca, N., Terrier, F., & Vincenti, F. The potential of MR Imaging in post-transplant renal failure. *Radiology*, 1984, 153, 59.
54. Höglund, A., & Odeblad, E. Sperm penetration in cervical mucus: A biophysical and group-theoretical approach. In *The uterine cervix in reproduction* V. Insler & G. Bettendorf (eds.), Stuttgart: Georg Thieme Publishers, 1977, 129–34.
55. Inouye, T., Satoh, K., Kose, K., & Yamakawa, K. Methods for relaxation time computed images. *Proceedings of the 3rd Annual Meeting of the Society of Magnetic Resonance in Medicine*, 1984, 371.

56. Kaufman, L., Crooks, L., Sheldon, P., Hricak, H., Herfkens, R., & Bank, W. The potential impact of nuclear magnetic resonance imaging on cardiovascular diagnosis. *Circulation*, 1983, 67, 251–57.
57. Kneeland, J. B., Kazam, E., Caputo, T., Knowles, J. R., & Cahill, P. T. Comparison of MR imaging and CT/ultrasound imaging of gynecologic tumours. *Radiology* 1984, 153, 32.
58. Knight, W. D. Nuclear magnetic shift in metals. *Physiology Review*, 1949, 76, 1259–60.
59. Lauterbur, P. C. Image formation by induced local interaction: Examples employing NMR. *Nature*, 1973, 242, 190–91.
60. Li, K. C., Henkelman, R. M., Poon, P. Y., & Rubenstein, J. Magnetic resonance imaging of the normal knee. *Proceedings of the 3rd Annual Meeting of the Society of Magnetic Resonance in Medicine*, 1984, 473.
61. Lipuma, J. P., Bryan, P. J., Butler, H. E., Dandrea, Miraldi, F. D., & Hau, T. Renal transplant MR: A Prospective study. *Radiology*, 1984, 153, 59.
62. Mansfield, P. Multiplanar image formation using NMR spin echoes. *Journal Phys C Solid State Phys*, 1977, 10, 55–8.
63. Mansfield, P., Pykett, I. L., Morris, P. G., & Coupland, R. E. Human whole body line-scan imaging by NMR. *British Journal of Radiology*, 1978, 51, 921–22.
64. Mendonca-Dias, M. H., Gaggelli, E., & Lauterbur, P. C. Paramagnetic contrast agents in nuclear magnetic resonance medical imaging. *Sem Nucl Med* 1983, 13, 364–76.
65. Mills, C. M., Crooks, L. E., Kaufman, L., & Brant-Zawadzki, M. Cerebral abnormalities: Use of calculated T1 and T2 magnetic resonance images for diagnosis. *Radiology*, 1984, 150, 87–94.
66. Moon, R. B., & Richards, J. H. Determination of intracellular pH by phosphorous NMR. *Journal of Biological Chemistry*, 1973, 248, 7276–78.
67. Newman, R. J., Bore, P. J., Chan, L., Gadian, D. G., Styles, P., Taylor, D., & Radda, G. K. NMR studies of forearm muscle in Duchenne dystrophy. *British Medical Journal*, 1982, 284, 1072.
68. NRPB (National Radiological Protection Board) (Great Britain). Exposure to nuclear magnetic resonance clinical imaging. *Radiography*, 1981, 47, 258–60.
69. NRPB (National Radiological Protection Board) (Great Britain). Revised guidance on acceptable limits of exposure during nuclear magnetic resonance clinical imaging. *British Journal of Radiology*, 1982, 56, 974–82.
70. Odeblad, E., & Lindström, G. Some preliminary observations on the NMR in biological samples. *Acta Radiologica*, 1955, 43, 469–76.
71. Olsson, M., Persson, B. R. R., Salford, L. G., & Schröder, U. The use of paramagnetic and ferromagnetic substances as contrast agent in NMR-imaging of T1 and T2 respectively. In *Magnetic Resonance Imaging and Spectroscopy*. M. A. Hopf & G. M. Bydder (eds.), Geneva, Switzerland: European Society for Nuclear Magnetic Resonance in Medical Biology, 1985.
72. Ortendahl, D. A., Hylton, N. M., Kaufman, L., & Crooks, L. E. Tissue type identification with MRI using characteristic tissue parameters and hierarchical processing. *Proceedings of the 3rd Annual Meeting of the Society of Magnetic Resonance in Medicine*, 1984, 567–68.
73. Patric, J. L., & Haacke, E. M. Accuracy of computed T1 and T2 techniques. *Proceedings of the 3rd Annual Meeting of the Society of Magnetic Resonance in Medicine*, 1984, 572–73.
74. Procter, W. G., & Yu, F. C. The dependence of a nuclear magnetic resonance frequency upon chemical compound. *Physics Review*, 1950, 77, 717.
75. Purcell, E. M., Torrey, H. C., & Pound, R. V. Resonance absorption by nuclear magnetic moments in a solid. *Physics Review*, 1946, 69, 37–38.

76. Revel, D., Terrier, F., Hricak, H., & Higgins, C. B. Determination of the nature of pleural effusions with MR imaging. *Radiology*, 1984, 153, 209.
77. Rholl, K. S., Lee, J. K. T., Ling, D., Sicard, G., & Griffith, R. Differentiation of acute renal rejection and acute tubular necrosis: MR demonstration. *Radiology*, 1984, 153, 59.
78. Rinck, P. A., Petersen, S. B., Heidelberger, E., Acuff, V., Reinders, J., Bernardo, M. L., Hedges, L. K., & Lauterbur, P. C. NMR ventilation imaging of the lungs using perfluorinated gases. *Proceedings of the 2nd Annual Meeting of the Society of Magnetic Resonance in Medicine*, 1983, 302–3.
79. Runge, V. M., Stewart, R. G., Clanton, J. A., Jomes, M. M., Lukehart, C. M., Partain, C. L., & James, A. Work in progress, Potential oral and intraveneous paramagnetic NMR contrast agents. *Radiology*, 147, 789–91.
80. Sattin, W., Fitzgerald, L. T., Mareci, T. H., & Scott, K. N. Determination of T1 by NMR imaging in an inhomogeneous Rf field. *Proceedings of the 3rd Annual Meeting of the Society of Magnetic Resonance in Medicine*, 1984, 654–55.
81. Schörner, W., Felix, R., Claussen, C., Laniado, M., Niendorf, H. P., & Weinmann, NMR-imaging of brain tumours with gadolinium-DTPA in humans. *Proceedings of the 3rd Annual Meeting of the Society of Magnetic Resonance in Medicine*, 1984, 665–66.
82. Sepponen, R. E., Sipponen, J. T., Tanttu, J. I. A method for chemical shift imaging: Demonstration of bone marrow involvement with proton chemical shift imaging. *Journal of Computer Assisted Tomography*, 1984, 8, 585–87.
83. Sepponen, R. E. Personal communication, Helsinki, Finland 1984.
84. Singer, J. R. Blood-flow rates by NMR measurement. *Science*, 1959, 130, 1652–53.
85. Starck, D. D., McCarthy, S. M., Callen, P. W., Hricak, H., & Filly, R. A. MR imaging of intrauterine growth retardation. *Radiology* 1984, 153, 31.
86. Stelling, C. B., Wang, P. C., Lieber, A., Mattingly, S. S., Griffen, W. O., & Powell, D. E. MR imaging of the female breast using a prototype breast coil. *Radiology*, 1984, 153, 163.
87. Stein, A. A., Lakshiminarayanan, A. V., & Gangarosa, R. E. Application of artificial intelligence to NMR clinical evaluation. *Proceedings of the 3rd Annual Meeting of the Society of Magnetic Resonance in Medicine*, 1984, 702–3.
88. Technicare (1984) Figures from work in progress on "Flow imaging and two component chemical shift imaging." Technicare Corporation, Cleveland, Ohio.
89. Thomas, S. R., Clark, Jr., L. C., Ackerman, J. L., Pratt, R. G., Hoffmann, R. E., Kinnett, D. G., & Kinsey, R. A. NMR imaging of the lung using liquid perfluorocarbon. *Proceedings of the 3rd Annual Meeting of the Society of Magnetic Resonance in Medicine*, 1984, 702–3.
90. Turner, D. A., Prodromos, C. C., & Clark, J. W. MR imaging in detecting acute injury of ligaments of the knee. *Radiology*, 1984, 153, 115.
91. Vinocur, B. Tapping into blood flow with magnetic resonance. *Diagnostic Imaging*, 53, 48–52.
92. Wang, P. C., Stelling, C. B., Mattingly, S. S., & Powell, D. E. *In vivo* breast magnetic resonance imaging using a prototype breast coil. In Esser & Johnston (eds.) *Technology of NMR* Society of Nuclear Medicine of New York, 1984, 179–91.
93. Wehrli, F. W., Shimakawa, A., MacFall, J. R., Axel, L., & Perman, W. H. Blood-flow velocity mapping in arteries and veins. *Radiology*, 1984, 153, 63.
94. Weinreb, J. C., Lowe, T. W., Santos-Ramos, R., Parkey, R. W., Cunningham, F. G., & Nunnally, R. The role of MR imaging in obstetrical diagnosis. *Radiology*, 1984, 153, 31.
95. Witcofski, R. L., Karstaedt, N., Partain, L., eds. *NMR imaging: Proceedings of an international symposium in NMR imaging*. Oct. 1–3, 1981. Bowman Gray School of Medicine of Lake Forest University, Winston-Salem, North Carolina.

96. Wolfman, N. T., Moran, P. R., & Moram, R. Dedicated MR receiver coil allowing simultaneous breast imaging. *Radiology*, 1984, 153, 163.
97. Yoon, Y. S., Makley, J. T., Benson, J. E., Han, J. S., & Alfidi, R. J. MR imaging of bone tumors. *Radiology*, 1984, 153, 213.
98. el Yousef, S. J. Magnetic resonance imaging of the human breast: Comparative evaluation with mammography. *Proceedings of the 3rd Annual Meeting of the Society of Magnetic Resonance in Medicine,* 1984, 772–73.
99. Zimmerman, R. D. MRI in vascular abnormalities of the brain. *Proceedings of the 3rd Annual Meeting of the Society of Magnetic Resonance in Medicine*, 1984, 783.

https://doi.org/10.1017/S0266462300001501 Published online by Cambridge University Press

SECOND ANNUAL MEETING

International Society for Technology Assessment in Health Care

May 30 - 31, 1986
National Academy of Sciences
Washington, D.C.

SPECIAL SESSIONS - INVITED PAPERS:

- **Forecasting Medical Technology**
- **Presentation on the Council on Health Care Technology**

CONTRIBUTED PAPER SESSION:

Abstracts have been solicited to cover topics such as results of specific technology assessments, analyses of interactions between people and technology, technology as a force in social and organizational change, and technology as it is created, produced, applied, and paid for.

KEYNOTE SPEAKER

SOCIETY BUSINESS MEETING

POST-MEETING SITE VISITS FOR NON-U.S. ATTENDEES:

Sessions are being arranged at agencies and institutions involved in technology assessment in Washington, Baltimore, Philadelphia, and Boston during the week of June 2-5.

A summary of the scientific program will appear in the *International Journal of Technology Assessment in Health Care* following the meeting.

The meeting is being held in cooperation with the World Health Organization.

For meeting information, contact:

Seymour Perry, M.D.
Institute for Health Policy Analysis
2121 Wisconsin Avenue, NW, Suite 220
Washington, D.C. 20007
U.S.A.
(202) 625-2115